

Scanning probe microscopy with inherent disturbance suppression

A. W. Sparks^{a)} and S. R. Manalis^{b)}

Massachusetts Institute of Technology, Media Laboratory, 20 Ames Street, Cambridge, Massachusetts 02139

(Received 16 June 2004; accepted 13 September 2004)

We introduce a general approach for inherently suppressing out-of-plane disturbances in scanning probe microscopy that enables higher-resolution imaging, particularly in noisy environments. In this approach, two distinct sensors simultaneously measure the probe-sample separation. One sensor measures a spatial average over a large sample area while the other responds locally to topography underneath the nanometer-scale probe. When the localized sensor is used to control the probe-sample separation in feedback, the spatially distributed sensor signal reveals only topography. We implemented this approach on a scanning tunneling microscope using a microcantilever with an integrated tunneling tip and interferometer. For disturbances applied normal to the sample, we measure -50 dB of disturbance suppression at 1 Hz, compared to 0 dB with conventional imaging. © 2004 American Institute of Physics. [DOI: 10.1063/1.1812377]

Scanning probe microscopes are notoriously susceptible to disturbances, or mechanical noise, from the surrounding environment that couple to the probe-sample interaction. These disturbances include vibrations of mechanical components as well as piezo drift and thermal expansion. Disturbance effects can be substantially reduced by designing a rigid microscope, incorporating effective vibration isolation, and selecting an appropriate measurement bandwidth and image filter. However, it is not always possible to satisfy these requirements sufficiently, and as a result, critical features in an image can be obscured.

The central problem is that the actuator signal, measured at the output of the feedback controller, is used both to read-out topography and correct for disturbances. Abraham *et al.*¹ demonstrated disturbance suppression for scanning tunneling microscopy (STM) with an ac modulation technique that measures differential topography. However, the true topography depends on the work function² and requires image reconstruction.³ Schitter and Stemmer⁴ attached an auxiliary sensor to an atomic force microscope (AFM) and subtracted its signal from the actuator signal. While straightforward to implement, performance of this approach is ultimately governed by the degree of coherence, or similarity, between the disturbance responses of the probe-sample sensor and the auxiliary sensor. Furthermore, the two responses must be subtracted with extreme precision in order to achieve a high common-mode rejection ratio.

Here we introduce a general approach for inherently suppressing out-of-plane (Z) disturbances in scanning probe microscopy (SPM). In this approach, two distinct, coherent sensors simultaneously measure the probe-sample separation. One sensor measures a spatial average distributed over a large sample area while the other responds locally to topography underneath the nanometer-scale probe. When the localized sensor is used to control the probe-sample separation in feedback, the distributed sensor signal reveals only topog-

raphy. This configuration suppresses disturbances normal to the sample. We apply this approach to STM with a microcantilever that integrates a tunneling tip and an interferometer, and we show that it enables Angstrom resolution imaging of nanometer-sized gold grains in a noisy environment. For disturbances applied normal to the sample, we measure disturbance suppression of -50 dB at 1 Hz, compared to 0 dB with conventional imaging.

Figure 1 illustrates Z disturbance suppression with this technique. One sensor (blue) is localized to an area smaller than the sample features, and is therefore sensitive to the topography. The other sensor (red) distributes this measurement over an area much larger than the features, making it insensitive to sample topography. When the feedback loop is closed around the localized sensor, the Z actuator will correct for Z disturbances. These corrections will appear in the actuator signal but not at the output of either sensor. During XY scanning, the actuator will make additional corrections for topography, which will therefore not appear at the localized sensor output. However, these topography corrections originate from changes that the distributed sensor cannot detect. As a consequence, the distributed sensor will reveal the sample topography. Therefore, within the feedback band-

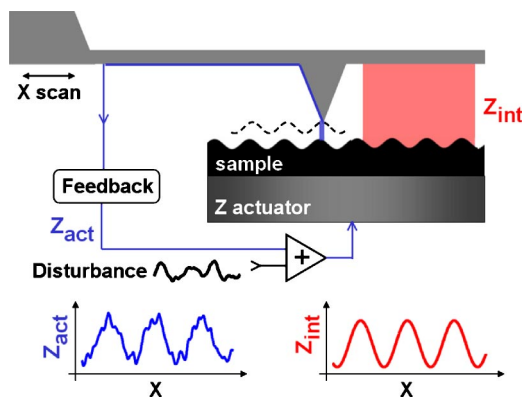


FIG. 1. (Color online). Operation schematic for inherent disturbance suppression in a scanning probe microscope. The red distributed sensor signal, z_{int} , reveals only topography while the actuator signal, z_{act} , includes both topography and disturbances. The actuator signal is defined as the controller output, and disturbances are modeled as signals added to the actuator output.

^{a)}Also at: Department of Materials Science and Engineering, Massachusetts Institute of Technology, Cambridge, MA 02139.

^{b)}Also at: Division of Biological Engineering, Massachusetts Institute of Technology, Cambridge, MA 02139; electronic mail: scottm@media.mit.edu

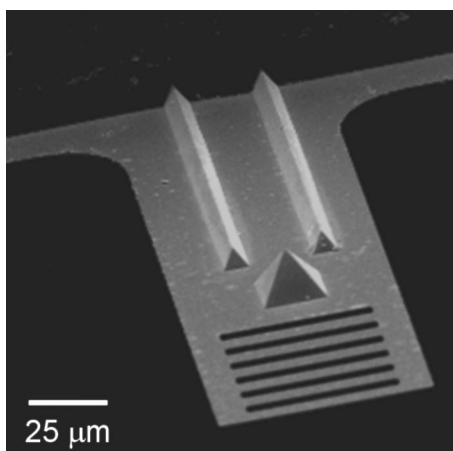


FIG. 2. Scanning electron micrograph of the silicon nitride cantilever with integrated tunneling probe and interferometer. The cantilever resonant frequency is 70 kHz, and the spring constant at the tunneling tip is estimated to be 30 N/m.

width, the distributed sensor shows only topography, the actuator signal shows topography and disturbances (as in conventional SPM imaging), and the localized sensor shows neither. Disturbance suppression is inherent and no subtraction is necessary.

A scanning electron micrograph of a silicon nitride cantilever with a localized tunneling probe and a distributed interferometer is shown in Fig. 2. The interferometer consists of an array of slits that is illuminated with a focused laser beam while an optically flat sample is scanned underneath the cantilever. Light traveling through the slits reflects from the sample and interferes with light reflected from the cantilever, creating a phase sensitive diffraction grating.⁵ The probe-sample separation is determined by measuring the intensity of a diffracted mode,⁶ which varies sinusoidally with separation.⁷ Due to the spot size of the laser, the resulting separation measurement is an effective average over an area of typically $500 \mu\text{m}^2$. The tunneling probe, on the other hand, measures the separation over as little as 1nm^2 .⁸ Both sensors measure the separation between the sample and a particular location along the cantilever. Although these cantilever locations differ for each sensor, they are rigidly connected to ensure high Z coherence between the two sensor signals. Since interaction forces between the probe and sample can be quite large,⁹ two hollow, longitudinal “fins” were used to stiffen the cantilever by increasing its effective thickness. The cantilever is fabricated by a well-established process where the tip and fins are simultaneously defined by etching silicon anisotropically with potassium hydroxide.¹⁰ Cantilevers are subsequently coated with an electron-beam evaporated Ti/Pd/Au multilayer film for tunneling and reflectivity purposes.¹¹

All measurements were performed on a home-built STM that was not optimized for vibration isolation or mechanical rigidity. The cantilever and sample were magnetically mounted on a Z piezo stack (Thorlabs, AE0203D04) and XY unimorph scanner,¹² respectively. Tunneling current was detected with a commercial current amplifier (RHK, IVP-200). A simple analog integral controller was used to stabilize the tunneling current. The controller output, or actuator signal, was amplified by a power amplifier before driving the actuator. The feedback bandwidth was limited to below 1 kHz by the Z resonance of the XY scanner. Light from a diode laser

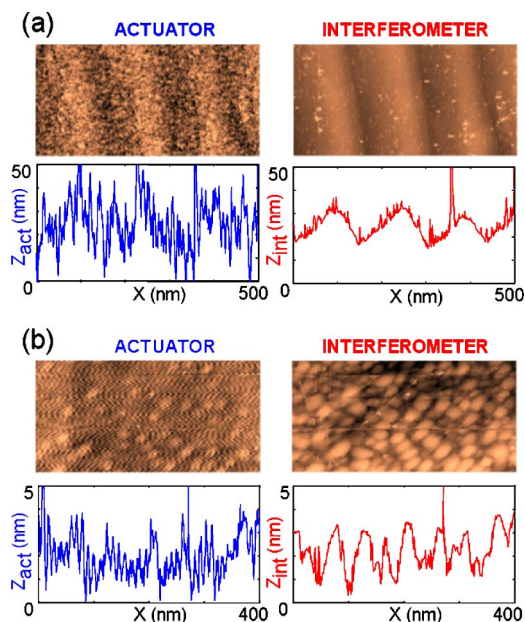


FIG. 3. (a) (Color online). $500 \times 250 \text{nm}^2$ images of a gold sawtooth calibration grating, scanned at 0.5 Hz, in the presence of a synthesized disturbance. The disturbance was created by filtering a white-noise source with a first-order 35 Hz low-pass filter and adding it to the actuator signal. The left image shows the actuator signal z_{act} after planefit, and the right image shows the raw interferometer signal z_{int} (no planefit). Cross sections are included for the same scan line. (b) $400 \times 200 \text{nm}^2$ images of Au/Pd/Ti on a silicon substrate. A noisy environment was created by mechanically grounding the optics table while the sample was imaged at a scan rate of 0.2 Hz. Cross sections from each image are shown for the same scan line.

was focused onto the cantilever slits with an achromatic lens, and the diffracted mode intensity was measured with a large-area reverse-biased photodiode (Thorlabs, DET110). The short optical pathlength difference of the $15 \mu\text{m}$ deep grating minimizes effects of refractive index fluctuations in air and phase noise of the laser that limit the resolution of interferometers. Both the sample and the lens were mounted on three-axis translation stages. We have found the interferometer readout to be insensitive to vibrations of the laser, lens, and photodiode. The entire assembly was covered in an acoustically isolating box on a floating optics table.

The system was engaged in tunneling feedback with a computer-controlled stepper motor. Because of the nonlinear dependence of the mode intensity on separation, the interferometer was biased at a point of maximum slope to achieve maximum sensitivity. This bias was adjusted in tunneling feedback either by moving the laser spot position on the grating or by changing the XY offset of the sample relative to the tunneling probe. The actuator and interferometer signals were processed by antialiasing filters before being recorded by LabView. Images from the actuator signal were planefit offline to remove effects of sample tilt. This operation was not necessary for the interferometer signal, allowing image acquisition at higher signal gain. The interferometer signal was calibrated either from the known response of the Z piezo or by relating the displacement response of the interferometer to the wavelength of illumination.¹³

Figure 3(a) shows images of a gold sawtooth calibration grating that were acquired in the presence of a synthesized disturbance. This disturbance was created by filtering a white-noise source with a first-order 35 Hz low-pass filter and adding it to the actuator signal. On the left, the actuator

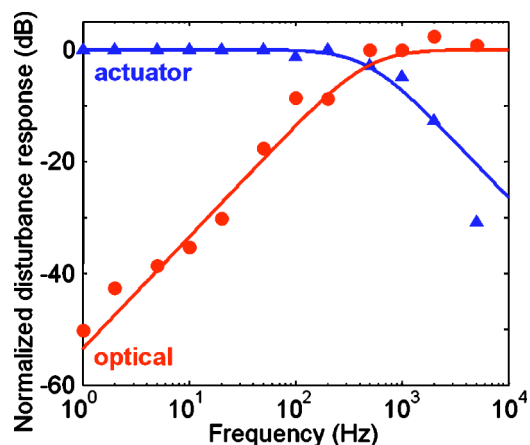


FIG. 4. (Color online). Disturbance suppression of the microscope, excited by a synthesized sinusoidal disturbance and measured by a lock-in technique. The curves are fit using classical feedback theory for a loop with dynamics only from an integrator.

signal shows the signature of the disturbance to the extent that the grating lines are barely visible. On the right, the interferometer signal shows strong suppression of the noise, especially at low frequencies, and allows clear identification of the sawtooth profile. In Fig. 3(b), the synthesized disturbance is turned off and a flat gold film was imaged while the optics table was mechanically grounded. Exposed to fourth floor building vibrations and with ten times less topography than the calibration grating, many grains are unresolvable in the actuator signal. The interferometer signal, however, reveals them with clarity.

To quantify the suppression performance of this system without the effects of sensor noise, we created single frequency disturbances by adding a sinusoidal voltage to the actuator signal. These disturbances were kept between 10 and 50 nm, well above the noise floor of the sensors but within the linear operating regime of the interferometer. Both actuator (blue) and interferometer (red) signals were monitored by lock-in amplifiers; their steady-state amplitudes are recorded in Fig. 4. Curves were fit using classical feedback theory for a simplified feedback loop with only an integrator, gain, and a closed-loop bandwidth of 500 Hz.¹⁴ Disturbance suppression of -50 dB was achieved at 1 Hz, the lowest frequency measured. This value increased linearly with frequency up to the feedback bandwidth and will decrease linearly with increasing bandwidth.

It is important to note that higher-resolution images on this microscope were not possible due to disturbances in X and Y . As a result, small features, especially when acquired at slow scan rates, tended to be smeared out. However, by incorporating this device into a more stable and better isolated microscope, we can expect image resolution to be limited only by the noise of the interferometer, estimated at

0.02 \AA in a bandwidth of 10 Hz–1 kHz,⁶ and the noise of the tunneling process, estimated at less than 0.1 \AA in the same bandwidth.^{1,2} Such a microscope would have lateral resolution comparable to a conventional STM but maintain the same high suppression in Z that we have achieved in this work. Furthermore, this instrument could be developed for a complementary application: interferometric feedback with tunneling readout, enabling closed-loop, constant-height tunneling spectroscopy. This previously unattainable mode could allow chemical identification on the molecular scale in a variety of experimental conditions, including aqueous environments.

We also suggest the extension of this technique to other noncontact variants of SPM, namely tapping mode and non-contact AFM. In these applications, a single interferometer could provide both the localized signal (high-frequency oscillation amplitude) as well as the distributed signal (offset). This would extend the application of inherent disturbance suppression to a wider range of samples with little added complexity.

This work was supported by Air Force Office of Sponsored Research (AFOSR) F49620-02-1-0322 and the National Science Foundation (NSF) Center for Bits and Atoms Contract No. CCR-0122419. The authors thank Cagri Savran and Thomas Burg for experimental advice and Paul Benning for helpful comments on the manuscript. The grating samples were kindly provided by the research group of Mark Schattenburg. One of the authors (A. W. S.) acknowledges partial support from a National Defense Science and Engineering Graduate Fellowship. Microcantilever devices were fabricated in the MIT Microsystems Technology Laboratories.

¹D. W. Abraham, C. C. Williams, and H. K. Wickramasinghe, *Appl. Phys. Lett.* **53**, 1503 (1988).

²S. Sugita, Y. Mera, and K. Maeda, *J. Appl. Phys.* **79**, 4166 (1996).

³E. P. Stoll and J. K. Gimzewski, *J. Vac. Sci. Technol. B* **9**, 643 (1991).

⁴G. Schitter and A. Stemmer, *Nanotechnology* **13**, 663 (2002).

⁵O. Solgaard, F. S.A. Sandejas, and D. M. Bloom, *Opt. Lett.* **17**, 688 (1992).

⁶S. R. Manalis, S. C. Minne, A. Atalar, and C. F. Quate, *Appl. Phys. Lett.* **69**, 3944 (1996).

⁷N. A. Hall and F. L. Degertekin, *Appl. Phys. Lett.* **80**, 3859 (2002).

⁸P. K. Hansma and J. Tersoff, *J. Appl. Phys.* **61**, R1 (1987).

⁹D. Ertz, A. Lohmus, R. Lohmus, H. Olin, A. V. Pokropivny, L. Ryen, and K. Svensson, *Appl. Surf. Sci.* **188**, 460 (2002).

¹⁰T. R. Albrecht, S. Akamine, T. E. Carver, and C. F. Quate, *J. Vac. Sci. Technol. A* **8**, 3386 (1990).

¹¹T. W. Kenny, W. J. Kaiser, H. K. Rockstad, J. K. Reynolds, J. A. Podosek, and E. C. Vote, *IEEE J. MEMS* **3**, 97 (1994).

¹²J. D. Alexander, http://www.geocities.com/spm_stm/Project.html

¹³G. G. Yaralioglu, A. Atalar, S. R. Manalis, and C. F. Quate, *J. Appl. Phys.* **83**, 7405 (1998).

¹⁴G. F. Franklin, J. D. Powell, and A. Emami-Naeini, *Feedback Control of Dynamic Systems*, 3rd ed. (Addison-Wesley, Reading, Mass., 1994).